Conf-950344--5 SAND94-0951C

# A MICROSTRUCTURALLY BASED MODEL OF SOLDER JOINTS UNDER CONDITONS OF THERMOMECHANICAL FATIGUE

D. R. Frear, S. N. Burchett Sandia National Laboratories Albucusmue, NM

ൾ. %. ിമടർര് University of California, Davis Davis, CA

#### **ABSTRACT**

The thermomechanical fatigue failure of solder joints is increasingly becoming an important reliability issue. In this paper we present two computational methodologies that have been developed to predict the behavior of near eutectic Sn-Pb solder joints under fatigue conditions that are based on metallurgical tests as fundamental input for constitutive relations. The two-phase model mathematically predicts the heterogeneous coarsening behavior of near eutectic Sn-Pb solder. 'The finite element simulations from this model agree well with experimental thermomechanical fatigue tests. The simulations show that the presence of an initial heterogeneity in the solder microstructure could significantly degrade the fatigue lifetime. The single phase model is a computational technique that was developed to predict solder joint behavior using materials data for constitutive relation constants that could be determined through straightforward metallurgical experiments. A shear/torsion test sample was developed to impose strain in two different orientations. Materials constants were derived from these tests and the results showed an adequate fit to experimental results. The single-phase model could be very useful for conditions where microstructural evolution is not a dominant factor in fatigue.

#### INTRODUCTION

The reliability of electronic systems is becoming increasingly dependent upon the thermomechanical fatigue life of the soldered connections in electronic packages. Thermomechanical fatigue arises because the materials in the package have different coefficients of thermal expansion. When the soldered assembly encounters thermal fluctuations (due to internal heating or changes in ambient temperature) strain is imparted to the joint. Thermally induced cyclic strain is the primary degradation to reliability in solder interconnections.

The alloy most commonly used as an interconnect in electronic packaging is near eutectic 60Sn-40Pb solder. This alloy is used because its melting temperature of 183°C makes solder processing compatible with the other materials used in a package. The 60Sn-40Pb alloy also has good wetting behavior and bonds well to the copper metallizations typically used in electronics assembly.

The structure of the 60Sn-40Pb alloy is not homogeneous or isotropic, and deforms heterogeneously under thermomechanical fatigue conditions. The series of optical micrographs in Figure 1 shows the evolution of the solder microstructure at 10% shear strain and under a thermal cycle of -55° to 125°C. The deformation concen-

DISTRIBUTION OF THIS DOCUMENT IS UNLIMITED

# **DISCLAIMER**

Portions of this document may be illegible in electronic image products. Images are produced from the best available original document. trates at cell boundaries in the microstructure resulting in additional coarsening. Eventually, cracks form in these coarsened regions resulting in mechanical and electrical failure. In order to be able to ensure the reliability of a given electronic system, a thermomechanical fatigue life prediction methodology is needed.

A number of methodologies have been proposed to predict the lifetime of solder joints in thermomechanical fatigue. A summary, and critical review, of some of the more prevalent methodologies can be found elsewhere (Sandor, 1991; Solomon, 1993). In the last few years, a number of new models have been proposed and summaries of these new models are given here. A common shortfall of these methodologies is that they are empirical in nature and do not include the microstructural evolution that occurs in 60Sn-40Pb solder during thermomechanical fatigue.

# **Current Solder Lifetime Reliability Models**

The thermomechanical fatigue damage to solder interconnections is strain-based low cycle fatigue. Coffin (1954, 1969) and Manson (1953, 1960) independently derived a relationship between the number of cycles to failure as a function of applied elastic and plastic strains:

$$\Delta \gamma = \frac{\sigma'_f}{E} [2N_f]^b + \epsilon'_f [2N_f]^c \qquad \text{Eqn. (1)}$$

where b and c are constants that are experimentally derived,  $\Delta \gamma$  is the applied shear strain,  $\sigma_f$  and  $\epsilon_f$  are the fatigue ductility coefficients, and E is the elastic modulus. For solder joints, the plastic deformation dominates and relation (1) is simplified to:

$$N_f = \left[\frac{\Delta \gamma}{2\varepsilon'_f}\right]^{\frac{1}{c}}$$
 Eqn. (2)

Using relation (2), life can be estimated if the plastic strain is known and the constants can be experimentally derived.

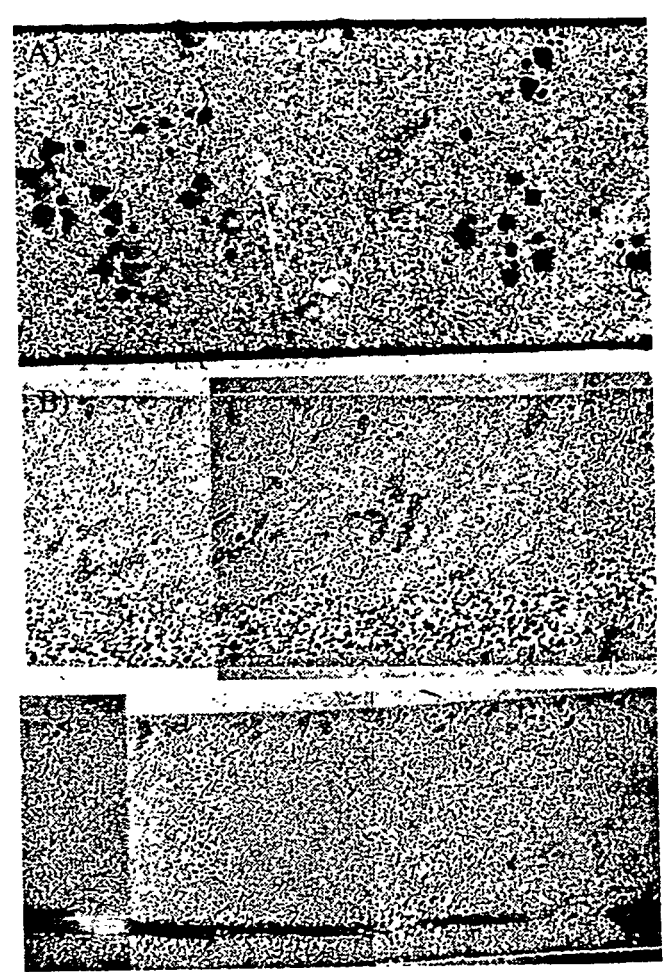


Figure 1 Heterogeneous coarsening in 60Sn-40Pb solder joints. A) As solidified, B) Heterogeneous coarsening, C) Failure through coarsened band.

A great deal of recent solder lifetime prediction modeling has been performed based on using the Coffin-Manson relation. This effort has focused on imposing the analytical determination of the strains, and stresses, in the solder joint by using improved finite element models. Once the stresses, or strains, are determined, the lifetime is predicted using an experimentally derived plot of strain versus the number of cycles to failure (a Coffin-Manson plot). Examples of these efforts include the following. Lau and Erasmus (1993) studied 304 pin Quad-Flat-Pack joints with constitutive relations derived assuming the solder is elastic-fully plastic. Sauber and Seyyedi (1992), used a power law creep equation in a finite ele-

ment simulation to calculate the solder joint creep response to time and temperature on leaded devices. Ross, et al. (1992) also modeled leaded devices and included both creep and creep ratcheting in the algorithm to determine stresses and strains in the solder joints. Schmidt (1992) developed a model of leadless solder joints based on a modified Coffin-Manson relation to determine the incremental deformation in the material which is summed to predict life using Miners rule.

A phenomenological model for solder joint life prediction has been proposed by a variety of workers (Verma, et al., 1993; Dasgupta, et al., 1992; Huang, et al., 1994) that is based on energy partitioning. In this methodology, the elastic, plastic and creep energy components are computed from an empirical fit of experimental test results that yeild a predicted hysteresis loop. Life is predicted using Miners rule from the accumulated damage to the joint in each cycle.

A reliability tool based on Figures of Merit has been developed to estimate fatigue life of solder joints (Clech et al. 1989). In the Figures of Merit approach, experimental data (such as isothermal fatigue lifetimes and lead compliances) are combined to compare one joint design with another using a series of formulas. This technique is accurate when there is sufficient field data to incorporate into the model. The technique is especially useful for considering small variations in design when the thermal environment is not severe. The methodology breaks down in severe thermal/mechanical environments and for designs where no empirical data exists. Further, there is no mechanism to incorporate microstructure into the tool.

Lau (1993) and Pao, et al., (1993) have proposed that fracture mechanics principles be used to determine the lifetime of solder joints. Pao and coworkers developed a constitutive relation based on creep and elastic deformation to model the behavior of 90Pb-10Sn solder joints and used the fracture mechanics relation of crack driving force, C\*, to model failure. They found fracture mechanics works well for large strains but underestimates life at small strains. Lau proposed a more radical use of fracture mechanics to predict the thermal fatigue life of solders using the stress intensity factor,  $\Delta K$ , and the Paris law to estimate the crack

growth rate in solder. Lau states that this use of fracture mechanics still requires a great deal of development due to the extensive assumptions needed to determine life.

The above life prediction techniques treat the solder as a homogeneous continuum and neglect the potentially large effects that the microstructure and heterogeneous deformation have on joint lifetime. A few models have been proposed recently to incorporate the microstructure in some form into the model. The constitutive relations developed by Akay, et al., (1993), Pan and Winterbottom (1990), Hacke, et al., (1993) and Busso, et al., (1994) incorporate materials constants purported to have the form of a grain or phase size. These constitutive relations are then used in a finite element code to predict stress and strain in the joints. Life is then predicted using an empirical Coffin-Manson relation. The effects of heterogeneities in the solder microstructure are discussed in the work of Guo, et al., (1992) who used a dislocation "pile-up" model as part of an effort to predict the deformation hysteresis loops in solder. The effect of the microstructure is incorporated indirectly because the dislocation pile-ups occur at phase and grain boundaries. Sandstrom, et al., (1993) also modeled the isothermal fatigue hysteresis loops of solder that used variations in the dislocation density to incorporate the inhomogeneous microstructure. The solder joint lifetime is predicted using a Coffin-Manson relation. The microstructure in the above models is static and there is no mechanism to include heterogeneities or microstructural evolution.

A reliability model that incorporates microstructure, heterogeneities, and microstructural evolution is needed to determine the lifetime of Sn-Pb solder joints under conditions of thermomechanical fatigue. In this paper we present methodologies that have been developed that use simplified experimental tests as fundamental input for two computational models to predict the behavior of the solder joints under deformation conditions. The important aspect of these methodologies is that they incorporate microstructure, and microstructural evolution, into the computer models.

#### **EXPERIMENTAL TECHNIQUES**

In the process of developing solder joint lifetime prediction models a number of experimental and computational techniques were developed. The following is a summary of the metallurgical experiments and techniques. The results of these tests were used as input to the computational models discussed later. The solder alloy used in these tests is near eutectic 60Sn-40Pb joined to copper substrates.

## **Metallurgical Experiments**

Thermomechanical Fatigue Tests. The thermomechanical fatigue tests have been performed in a simple shear orientation and provide results on microstructural evolution and solder joint lifetime. This procedure is described in greater depth elsewhere (Frear 1989, Frear, et al., 1993). A brief summary of the test method is given below.

The specimen used to test solder joints is shown in the schematic drawing in Figure 2. The specimen consists of 18 electrically isolated solder joints that, when the specimen is gripped and pushed and pulled on the ends, deform in shear. The joints have a simple truncated spherical geometry. Strain is imposed upon the solder joints by a servohydraulic load frame operated under strain control. Thermal fluctuations are induced by a chamber that fits around the specimen in the load frame. Compressed air is heated and cooled by a commercial heating and cooling system and circulates around the specimen. The strain and temperature are computer controlled. The temperature extremes tested were -55° to 125°C at 10% total shear strain. The thermal cycle consists of a ramp in strain and temperature to the elevated temperature extreme and a 3 minute hold period, a ramp down, and another 3 minute hold at the low temperature extreme. The deformation rate for this test was 2.1x10<sup>-4</sup>s<sup>-1</sup>. Failures are monitored electrically by monitoring spikes in resistance. The electrical data along with load, temperature, and strain are collected and stored on a computer. To examine the microstructure of the solder joints after testing, the samples were mounted and metallographically sectioned and polished to reveal the solder microstructure.

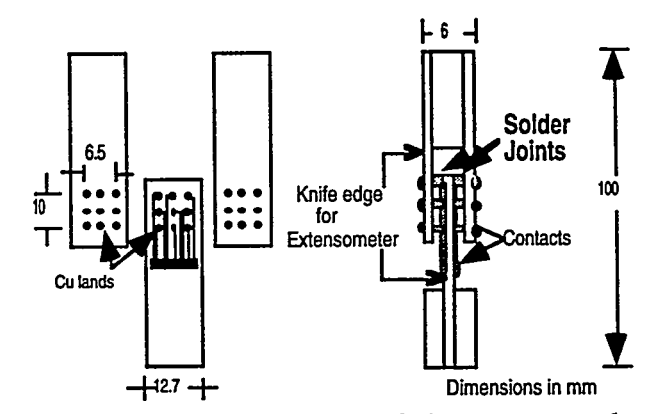


Figure 2 Thermomechanical fatigue test sample.

In Situ SEM Thermomechanical Fatigue Tests.

The microstructural evolution of the solder joints was examined in real time using an in situ SEM with a thermal/deformation stage (Frear et al. 1993). The system is shown in Figure 3. The SEM is equipped with a servohydraulic loadframe (inside the vacuum chamber) that can impose strain on a sample at a constant strain rate. The sample for this test has a single lap shear geometry with joint dimensions of 3.2mmx3.2mm. The grips that hold the solder joint samples can be heated and cooled and have an alignment feature that eliminates rotation in the single lap shear specimen. This test results in a real time observation of the thermomechanical deformation process of the solder microstructure. The SEM can be operated in secondary or backscatter mode. For Pb-Sn solder the difference in atomic weight is great so operating in backscatter mode clearly reveals the structure of the solder.

Shear/Torsion Testing of Solder Joints. Constitutive relation information for the single phase constitutive model was in part determined using a specially designed shear/torsion solder joint specimen shown schematically in Figure 4. The test sample has a "ring in plug" design where pulling along the z-axis results in shear deformation, and axial rotation causes shear deformation in an orientation 90° away from the z-axis. The samples were tested in a servo-hydraulic test frame

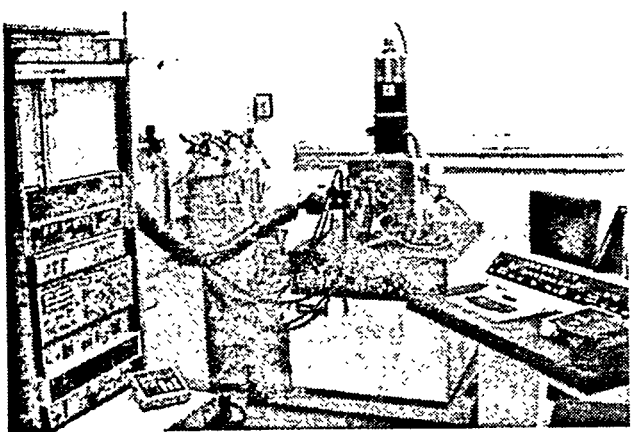


Figure 3 The in situ SEM test apparatus.

equipped with an electric rotational drive for torsion testing. Tests were performed at room temperature with the deformation cycle below:

**Table 1: Shear/Torsion Test** 

Rotation Rate (deg./sec.)	Deformation Rate (mm/sec.)	Time (seconds)
3x10 <sup>-4</sup>	0	600
0	3.6x10 <sup>-5</sup>	600
0	0	600
0	-3.6x10 <sup>-5</sup>	600
-3x10 <sup>-4</sup>	0	600
0	0	600

This results in a strain rate of  $1.0 \times 10^{-4} \text{sec}^{-1}$  for the entire test. A total of six cycles were imposed on each specimen and a total 8.48% shear strain amplitude. The data was collected digitally and plotted as load as a function of time.

## RESULTS AND DISCUSSION

Constitutive models were constructed and implemented into finite element simulations in order to predict solder joint behavior. Two different constitutive models have been formulated to describe the thermomechanical response of the 60Sn-40Pb solder alloy, and both are currently be-

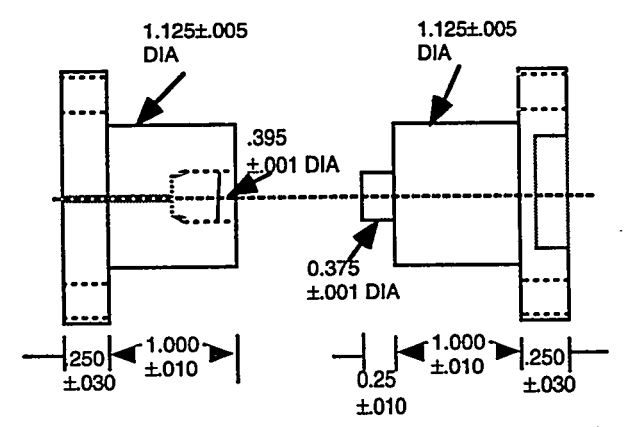


Figure 4 Shear/torsion test sample designed to impose two different orientations of shear strain onto a thin (0.254mm) solder joint. All dimensions are in mm.

ing used in a computational setting to compare theoretical predictions to experimental findings. The philosophy and intent underlying each of the two models are different: the two-phase model is intended to be used as a research tool by which the relative importance of certain microstructural phenomena may be evaluated. Microstructural evolution and mechanical behavior inputs to this model are derived from experimental thermomechanical fatigue tests on solder joints. On the other hand, the single-phase model is intended to render meaningful engineering predictions when used in a finite element code. In this simpler model, the emphasis is on striking a balance between representing complex microstructural phenomena, and limiting the number of empirically-determined parameters to a manageable number through analysis of experimental shear/torsion tests.

#### Two-Phase Model

In the two-phase model (Stone and Rashid, 1994), an attempt is made to mathematically represent the effects of the phase-region size in the tin-lead alloy. As mentioned previously, the characteristic size of the lead-rich phase regions has been observed to correlate strongly with strain localization and subsequent failure. In particular, local phase-region coarsening appears to be accompanied by a decrease in the overall flow resistance of the material, leading to an unstable concentration of strain and ultimately to fracture.

Whereas the model is intended to represent the effects of this coarsening phenomenon, the behavior of individual phase regions is not explicitly accounted for. Indeed, in "microstructurally motivated" material models such as this one, the model predictions are envisaged to correspond to a representative volume element of material that contains a statistically meaningful distribution of microstructural features. In concept, then, the physical material, with all its microscale heterogeneities, is represented by a replacement medium in which the important microstructural features (in this case, lead-rich phase regions) are present only in the material model itself. The material model involves state variables that characterize some statistical measure of the microstructure, and which generally vary smoothly in space. It is emphasized that the idea of a representative volume element does not constitute an analytical ingredient in a model of this type; rather, it is a conceptual guide in the model formulation.

The two-phase model retains separate average stress tensors  $\mathbf{T}^1$  and  $\mathbf{T}^2$  in the lead-rich and tinrich phases, respectively. Taking all rank-two tensors as deviatoric (without prime), each is governed by the evolution equation:

$$T^{\circ \alpha} = 2G_{\alpha}(D - \mu_{\alpha}T^{\alpha})$$
 Eqn. (3)

in which  $T^{\circ}$  indicates the Jaumann corotational rate, G the elastic shear modulus (elastic response taken to be isotropic), D the imposed stretching rate (i.e. symmetric part of the spatial velocity gradient), and  $\alpha=1$  or 2 specifies the phase. The overall Cauchy stress for the material element is obtained from the simple volume-average relation

$$T = fT^{1} + (1-f)T^{2}$$
 Eqn. (4)

in which f=0.40 and is the volume fraction of the lead-rich phase. Equations (3) and (4) represent the simplest possible means of modeling a mixture of two inelastic phases: each phase is assumed to exhibit simple isotropic viscoplastic behavior and suffer an identical imposed deformation rate, and the overall stress is obtained through a simple volume-weighted average. Any departure from these assumptions would involve considerable complication that is not warranted in this context.

The flow-rate parameters  $\mu_{\alpha}$  are taken to be giv-

en by the power-law expression:

$$\mu_{\alpha} = \frac{\dot{\varepsilon}_0}{\tau_{\alpha}} \left( \frac{\tau_{\alpha}}{\sigma_{\alpha}} \right)^{\frac{1}{M_{\alpha}}}$$
 Eqn. (5)

In (5),  $\tau_{\alpha} = (T_{ij}^{\alpha} T_{ij}^{\alpha})^{1/2}$  is the magnitude of the stress in each phase,  $\dot{\epsilon}_0$  is a constant with units inverse time, and  $M_{\alpha}$  is the rate-dependence exponent in each phase. The terms  $\sigma_{\alpha}$  are the values of the flow resistance in each phase, and are themselves subject to evolution laws that govern the hardening or softening behavior. In particular:

$$\sigma_{\alpha} = (\bar{\sigma}_{\alpha} + \hat{\sigma}_{\alpha}) \sigma_{\alpha}^{0}$$
 Eqn. (6)

$$\dot{\overline{\sigma}}_{\alpha} = C_1^{\alpha} \frac{\dot{\gamma}_{\alpha}}{\dot{\varepsilon}_0} - C_2^{\alpha} \left( \frac{\dot{\gamma}_{\alpha}}{\dot{\varepsilon}_0} \right)^{n_a} \overline{\sigma}_{\alpha} \qquad \text{Eqn. (7)}$$

$$\hat{\sigma}_{\alpha} = C_3^{\alpha} \left(\frac{\lambda}{\lambda_0}\right)^{-\frac{1}{2}}$$
 Eqn. (8)

$$\dot{\lambda} = \gamma_0 [fC_4^1 \dot{\gamma}_1 + (1 - f) C_4^2 \dot{\gamma}_2]$$
 Eqn. (9)

in which  $\dot{\gamma}_{\alpha} \equiv \mu_{\alpha} \tau_{\alpha}$  (equivalent plastic strain rate In phase).  $C_1^{\alpha}$ ,  $C_2^{\alpha}$ ,  $C_3^{\alpha}$ ,  $C_4^{\alpha}$ ,  $M_{\alpha}$ ,  $\sigma_{\alpha}^0$ ,  $n_{\alpha}$ ,  $\dot{\varepsilon}_0$  and  $\lambda$  are material constants, whereas  $\lambda$ ,  $\overline{\sigma}_{\alpha}$ , and  $\hat{\sigma}_{\alpha}$  are state variables. The term  $\overline{\sigma}_{\alpha}$  is intended to quantify the contribution of the dislocation network to flow resistance, and is therefore made to evolve with inelastic deformation; its evolution equation is written in hardening-recovery format as in Rohde and Swearengen (1980) and Busso et al. (1992). The term  $\lambda$  is a characteristic length associated with the phase-region size; its evolution equation is also related to a scalar measure of inelastic deformation rate as suggested by Arrowood et al. (1991). The parameter  $\hat{\sigma}_{\alpha}$  is defined directly by the Hall-Petch relationship (8), and is intended to quantify the effects of disruption of dislocation glide due to finite crystallite size.

Equations (3) - (9) completely specify the twophase constitutive model. This model has been implemented in a three-dimensional, large-deformation finite element code, and has been used to simulate some experiments performed on the tinlead near-eutectic solder alloy. A few of the results of these studies are presented below.

Thermomechanical fatigue tests were performed to examine the microstructural evolution and mechanical behavior of the solder joints. The results of in situ thermomechanical fatigue tests (-25 125°C and 10% total shear strain) are shown in Figure 5. Figure 5A is the as-solidified microstructure and 5B shows the structure after 25 cycycles the solder cles. Even after 25 microstructure has coarsened at the cell boundaries. The dark lines at the cell boundaries in Figure 5B are not cracks, they are artifacts of surface roughness. As the solder microstructure deforms the individual cells slide and rotate at the cell boundaries to accommodate the strain because the boundaries are the weakest part of the microstructure (Frear,1992). Observations by Lee (1993) showed that the surface of solder joints in electronic assemblies that have undergone thermomechanical fatigue revealed the sliding of eutectic cells and some surface crack initiation at the cell boundaries.

Examples of solder joints that have been thermomechanically fatigued, using the test geometry described above are shown in Figures 6 and 7. Both were tested at 10% shear strain at -55° to 125°C for 100 cycles. The sample in Figure 6 was tested at a deformation rate of  $5.6 \times 10^{-4} \, \text{s}^{-1}$  and the sample in Figure 7 was tested at a deformation rate of  $2.1 \times 10^{-4} \, \text{s}^{-1}$ . In Figure 6, the heterogeneous coarsened microstructure occurs adjacent to the bottom interface. In Figure 7, heterogeneous coarsening occurs throughout the microstructure at the cell boundaries.

To illustrate the effects of microstructural coarsening and to correlate with the experimental results discussed above (Figures 5-7), an example calculation was performed on a test specimen rep-

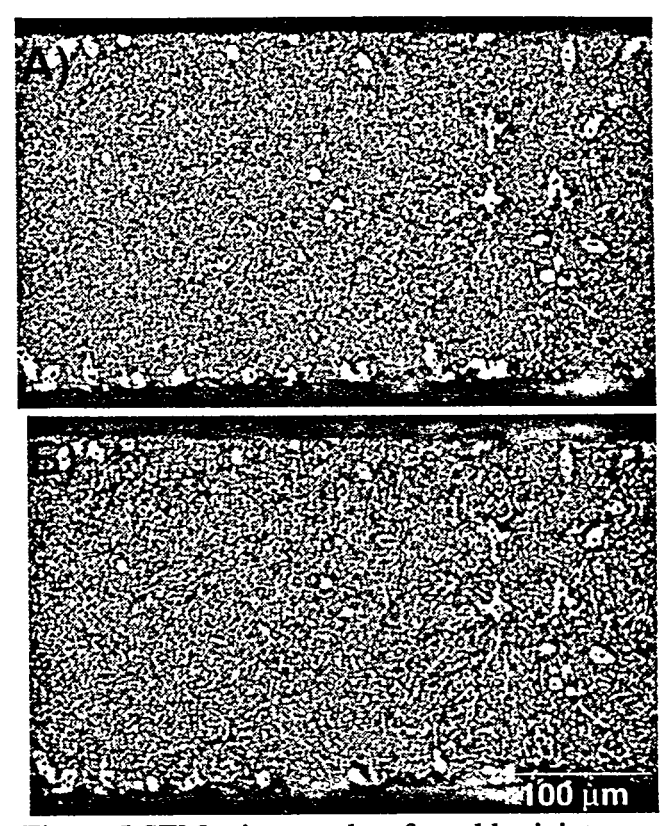


Figure 5 SEM micrographs of a solder joint using the *in situ* thermomechanical fatigue system. A) As solidified joint, B) after thermal cycling.

resentative of a simulated solder joint, (Figure 8). In this three-dimensional simulation, the 60Sn-40Pb solder was constrained between two copper platens which were modeled as elastic bodies. Cyclic shear displacement (Figure 9) was applied to the top surface of the upper copper platen while the bottom surface of the lower platen was restrained. The shear displacement approximates deformation due to thermal cycling in a typical solder joint, although the computation is isothermal. The magnitude of the shear displacement translates to approximately +/- 5% (total strain range =10%) shear strain in the solder joint. The strain rate assumed was 2.0x10<sup>-4</sup>/in. The material properties used for the two phase constitutive model discussed earlier are given in Table 2. The state variables used in the analysis were

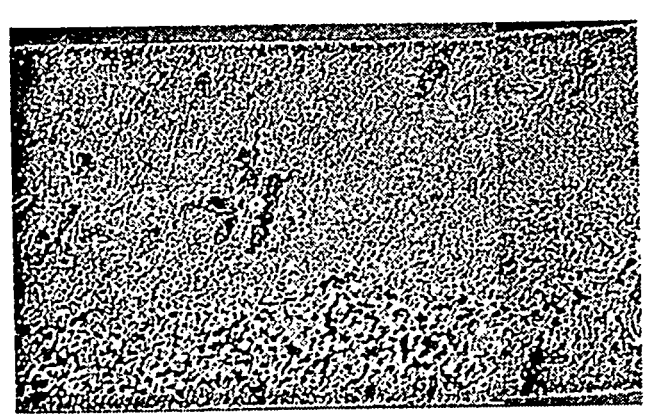


Figure 6 60Sn-40Pb solder microstructure after 100 thermal cycles and 10% shear strain and a deformation rate of 5.6x10<sup>-4</sup>s<sup>-1</sup>.

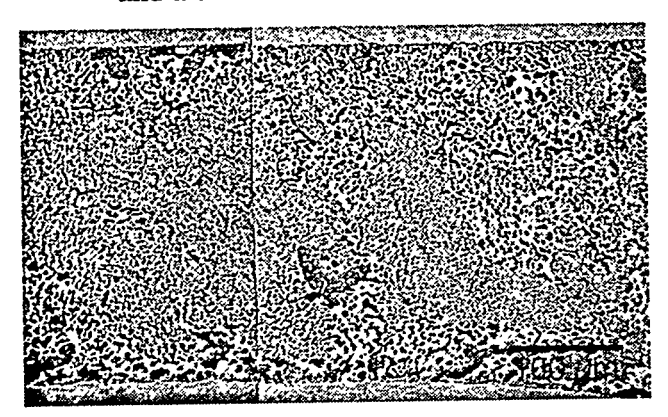


Figure 7 60Sn-40Pb solder microstructure after 100 thermal cycles and 10% shear strain and a deformation rate of 2.1x10<sup>-4</sup>s<sup>-1</sup>.

 $\lambda_0$ =1.0 $\mu$ m,  $\dot{\epsilon}_0$ =1.0min<sup>-1</sup>, and f=0.4.

**Table 2: Material Properties** 

Parameter	Lead-rich Phase	Tin-rich Phase
G	6.9 Gpa	13.8Gpa
В	15.2Gpa	30.3Gpa
M	0.3	0.1
$\sigma^0$	6.9Mpa	13.8Gpa
. C <sub>1</sub>	20.0	20.0
C <sub>2</sub>	100.0	100.0
C <sub>3</sub>	1.0	1.0
C <sub>4</sub>	10.0	10.0

Two computations were completed. In the first computation, the microstructure was assumed to initially be perfectly uniform. In Figure 10, the phase-size parameter at the end of six complete cycles is plotted. The results of this computation shows two bands where the microstructure coarsens; a dominant coarsened band near the top platen and a minor band near the bottom platen. At these locations, the material softens and strain is localized. These results compare favorably with observed microstructural coarsening for this geometry. The coarsening in this computation is precipitated by the shear strain variations in the solder.

In the second computation, the microstructure was assumed to be initially coarsened in the center of the solder joint. After six displacement cycles, the microstructural coarsening and strain localization in the center of the solder joint is substantially enhanced as shown in Figure 11.

In Figure 12, the maximum phase-size parameter is plotted as a function of time. The effect of initial microstructure is substantial. If one assumes that initial crack formation of the solder joint can be related to a specific grain size, the number of cycles to develop initial cracking would be substantially different, depending upon

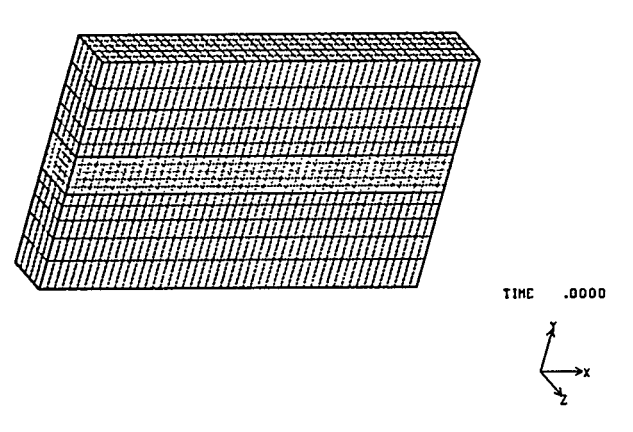


Figure 8 Meshed solder joint for two-phase finite element simulation.

APPLIED DISPLACEMENT

# 

Figure 9 Applied displacement versus time used for the two-phase finite element simulation.

initial microstructure. The number of cycles to failure would be substantially less if no initial coarsened band was present in the as solidified microstructure. It must be stated that the material properties and parameters used have not been adequately fit to 60Sn-40Pb solder and the model at the present time is not temperature dependent. These computations do, however, indicate that the two-phase model simulates the microstructural response of solder joints in thermomechanical fatigue conditions.

Despite the numerous simplifications and assumptions that have been made in arriving at

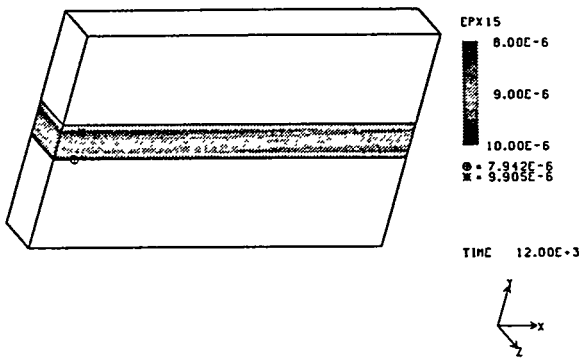


Figure 10 Finite element simulation results for a uniform initial microstructure. Note that heterogeneous coarsening occurs near the solder/copper interface.

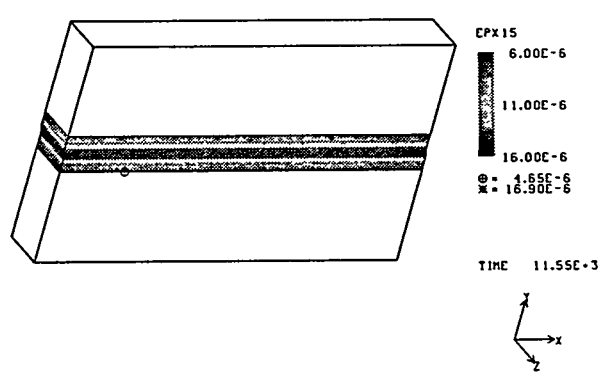


Figure 11 Finite element simulation results for a microstructure with an initial coarsened structure in the center of the joint.

the two-phase model, it is clear that experimentally obtaining reliable values for the constants that appear in the model is a formidable task. In particular, it is unclear if values for the constants corresponding to the individual phases can be obtained from either tests performed on the pure elemental phases or the mixture itself. As mentioned previously, however, the role of this model is that of research tool: even without accurate estimates for the material parameters, the model is of some utility in assessing the validity of various failure-sequence hypotheses through numeri-

### **EFFECT OF STARTING MICROSTRUCTURE**

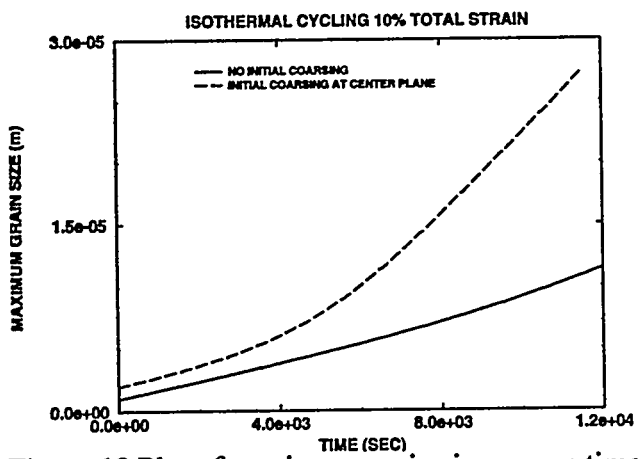


Figure 12 Plot of maximum grain size versus time for the finite element simulations that shows that an initially coarsned microstructure rapidly produces additional heterogeneous coarsened regions.

cal experimentation.

Single-Phase Model. In this model, no attempt is made to explicitly account for the microstructural coarsening effect. Rather, the simplest possible forms are chosen for the evolution equations in the model such that the important features of inelastic flow in the tin-lead near-eutectic alloy are represented. These forms are, in a sense, motivated by microscale considerations; however, this model's connection to microstructural observation is more tenuous than that of the previous model. The result is a model for which material parameter values may be reliably obtained from tests, and whose utility lies in facilitating engineering predictions made on the basis of finite element computations.

The single-phase model is based on the isotropic stress evolution equation:

$$T^{\circ} = 2G(D - \mu T)$$
 Eqn. (10)

which is identical in form to that used in each phase in the two-phase model. In constructing the flow rate function  $\mu$ , and in particular the manner in which it represents hardening, the following items were borne in mind:

- Inelastic flow in the alloys of interest, and in the temperature and strain-rate ranges of interest, is primarily due to dislocation motion, with relatively small contributions from diffusional mechanisms.
- Hardening is due to barriers to dislocation motion, such as immobile dislocations and phaseregion boundaries.
- The overall resistance to dislocation motion offered by the current pattern of barriers embodies the state of hardening; in this model it is quantified by a single scalar state variable.
  - Any real distribution of barriers is heterogeneously distributed on the submicron scale. For instance, immobile dislocations may organize themselves into a cellular structure, with cell interiors that are relatively free of dislocation debris. Certainly the arrangement of phase-region boundaries has a definite geometric structure. Accordingly, mobile dislocations will interact with these obstacles in a directionally-dependent manner. In particular, mobile dislocations may pile up against barriers, and when the stress direction is changed (or reversed), the resistance suffered by these piled-up dislocations may be significantly reduced. With regard to plasticity modeling, the usual conception of kinematic hardening involves the modification of the stress by subtracting from it a back stress, and then using the modified stress in a yield criterion or flow relation. This formulation corresponds most closely to grain-scale residual stresses as the mechanism responsible for directional hardening, as in metals at low homologous temperatures. However, in the case of solder, and more to the point, the high homologous temperatures at which it is used, it seems that large residual stresses on a small scale would relax quickly. Accordingly, the directional hardening is represented here as a modification to the isotropic flow resistance (i.e. the scalar hardening state variable mentioned above) rather than as a modification to the stress tensor itself. Indeed, this model is consistent with a simplified picture of the microscopic processes, in which the entire mobile dislocation network is subjected to a uniform stress. This network, however, may be interacting with the

pattern of obstacles in a directional manner, due to pile-ups.

 Due to thermal activation and the dislocationscale interaction stresses, both the immobile dislocation network, and any pile-ups of mobile dislocations, will tend to recover over time. The rate of recovery is enhanced by the application of stress. In the presence of stress, the recovery processes compete with the hardening processes.

The equations given below that define the scalar inelastic flow rate are the simplest possible forms that are consistent with the above qualitative statements. Whereas a "rigorous derivation" of a set of evolution equations based on the ideas listed above is, of course, not to be expected, it is important that the final model render predictions that are at least consistent with these assumed underlying mechanisms. The chosen form for the scalar inelastic deformation rate is:

$$\gamma = \varepsilon_0 \sinh^m \left[ \frac{\tau}{\alpha \Gamma \sigma} \right]$$
 Eqn. (11)

$$\dot{\sigma} = A_1 \gamma - A_2 (\sigma - \sigma_0) (1 + A_3 \gamma)$$
 Eqn. (12)

$$\Gamma = 1 + \frac{T}{\tau} \bullet B$$

$$\dot{B} = \gamma (A_4 \frac{T}{\tau} - A_4 B) - A_6 B \qquad \text{Eqn. (13)}$$

In (11) - (13),  $\gamma = \mu/\tau$  is a scalar measure of inelastic flow rate, and  $\alpha$  depends only on temperature. The rate-dependence relation (11) involves a hyperbolic sine function raised to a power, which was successfully used to fit a large amount of data by Darveaux and Banerji (1992). Consistent with the above discussion of dislocation pile-ups and the associated directionality of hardening, the scalar flow resistance is scaled by  $\Gamma$ , which is unity in the absence of directional hardening. The directional hardening is represented by the symmetric rank-two tensorial state variable **B** (similar to a back stress), which obeys the evolution equation given in (13). In the case of persistent unidirectional loading, **B** is coaxial with the Cauchy stress,

and saturates at a value of  $(A_4/A_5)T/\tau$  for fast loading processes. For lower strain rates, the  $A_6$  term in (13) (i.e. the recovery term) competes with the growth of **B**. In general, (13) is written so that **B** always tends toward the prevailing stress direction, and at a rate proportional to the inelastic flow rate, but with a recovery term that generally decreases the magnitude of **B**. The recovery can proceed in the absence of stress so long as the temperature is high enough, as it does in reality.  $\Gamma$  as given in (13) measures the extent to which **B** and the current stress are coaxial, and is used in (11) to modify the flow resistance that is experienced by the current pattern of mobile dislocations under the current stress state.

The first term in the evolution equation (12) for the scalar hardening parameter is a (linear) hardening term. The second term is a recovery term that competes with (and diminishes) the hardening in a nonlinear fashion. The  $\sigma_0$  is the annealed (or long-time-unstressed) flow resistance, and the term  $A_2(\sigma-\sigma_0)$  is the rate of recovery due to the dislocation interaction stresses. This rate of recovery can be accelerated by the application of stress (producing an inelastic flow rate), giving rise to the  $A_3\gamma$  term.

The material parameters are  $A_1$  -  $A_6$ ,  $\sigma_0$ ,  $\varepsilon_0$ , m, α, and two elastic constants. All of these constants are expected to be functions of temperature. At room temperature  $\alpha$  was set to unity, whereas  $\varepsilon_0$ was taken to be 1.0x10<sup>-4</sup> sec<sup>-1</sup>. A room-temperature value of m=3.3 taken from the work of Darveaux and Banerji (1992), as was the shear modulus  $G = 1.3 \times 10^4 \text{ MPa} (1.9 \times 10^6 \text{ psi})$ . The parameters  $A_1$  -  $A_6$  and  $\sigma_0$  were obtained by fitting the predicted stress response to the measured stress history in a tube-and-plug-type material test. In this test, a thin (0.254mm (0.010")) annular region of solder fills the gap between a tube and a plug, which may be subjected to a combination of shear and torsion. These two modes of deformation subject the sample to shear deformation in orthogonal directions. For the purposes of obtaining the required seven parameters the program of deformation in Table 1 was used. This pattern was repeated for a total of five cycles. This particular deformation path was chosen in order to probe not only the isotropic hardening behavior, but the directional hardening response as well. The deformation rates were specified so that the strain amplitude in each direction was roughly 0.05.

Because the stress response depends on the unknown parameters through the rate equations given above, the values of the parameters may not be obtained simply by, say, measuring a slope of a stress-strain curve. Indeed, the stress history over the entire deformation path depends on each of the parameters in a complex and highly coupled fashion. Accordingly, a conjugate-gradient-search procedure was used to aid in determining the values of the constants from the test data. In this procedure, a norm I is defined as:

$$I = \int_{t_1}^{t_1} \sqrt{(T_{13} - S_{13}) (T_{13} - S_{13}) + (T_{23} - S_{23}) (T_{23} - S_{23})} dt$$

Eqn. 14

which provides a scalar measure of the difference between the measured components of the experimental stress deviator **S**, and the computed stress deviator **T**. The gradient of **I** with respect to the seven unknown constants is computed by means of a perturbation technique. This gradient is subsequently used in a conjugate gradient algorithm to minimize the difference function **I**. In this way, the following values for the material constant were obtained (valid at room temperature):

$$\sigma_0$$
=3930 psi, A<sub>1</sub>=-1.261 psi, A<sub>2</sub>=-9.16x10<sup>-4</sup>s<sup>-1</sup>  
A<sub>3</sub>=1.33x10<sup>-3</sup>s<sup>-1</sup>A<sub>4</sub>=2.20, A<sub>5</sub>=0.218, A<sub>6</sub>=1.50x10<sup>-4</sup>s<sup>-1</sup>

These parameter values resulted in the fit shown in Figure 13 in which the solid lines are the experimental stress histories for both shear and torsion, and the dashed lines are the computed stress histories. The experimental curves were piece-wise fit using a third-order polynomial to determine the material constants for the single-phase model. The discrepancies observed during relaxation and unloading seem to arise from use of the Mises-type isotropic flow rule. Currently, various alternatives are being studied to improve the fit in these regimes.

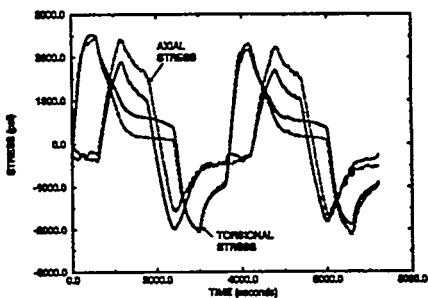


Figure 13 Plot of experimental shear/torsion test results with an overlay of the single-phase model prediction.

# **SUMMARY AND CONCLUSIONS**

Methodologies have been presented that use simplified experimental tests as fundamental input for two different computational models to predict the behavior of solder joints under conditions of thermomechanical fatigue.

The two phase model mathematically represents the effects of the phase-region size in the 60Sn-40Pb solder alloy and predicts the heterogeneous coarsening phenomenon of near-eutectic Sn-Pb solder under conditions of fatigue. Results of the two-phase model code showed good correlation with metallurgical experiments and showed that the presence of an initial heterogeneity in the solder microstructure accelerates the development of coarsening and could significantly reduce the fatigue life. The difficulty with this model is that deriving the material constants needed for the constitutive relation is a formidable task, in particular it is not clear whether the constants for the individual phases can be reliably obtained from tests on either the independent elemental materials or the mixture itself. However, this is model has utility assessing the validity of failure-sequence events of solder thermomechanical fatigue where microstructural evolution dominates failure.

The single-phase model was developed as a computational technique to predict the mechanical behavior, and eventually reliability, of solder joints using materials data that is readily available through metallurgical experiments. This technique could be very useful for conditions where microstructural evolution is not a dominant factor in fatigue. A shear/torsion test sample was developed to impose shear strains in two different ori-

entations to a solder joint. Constitutive relations were derived whose material constants could be determined through mathematical representation of shear/torsion test data. The predicted behavior shows adequate fit to the experimental results and various alternatives are being explored to develop a better fit. The promise shown in this technique is that the material constants needed for constitutive behavior input to finite element simulations may be determined through a series of easily performed experimental tests. This would thereby simplify the effort needed perform lifetime prediction through use of this engineering methodology.

#### **ACKNOWLEDGEMENTS**

The authors would like to acknowledge the experimental assistance of J. L. Finch and T. Rice for their work on the thermomechanical fatigue tests and S. Brandon for his work on the shear/torsion tests. This work was performed at Sandia National Laboratories, which is supported by the U. S. Department of Energy under contract number DEAC04-94AL85000.

#### REFERENCES

Akay, H. U., Tong, Y., Paydar, N., 1993, "Thermal Fatigue Analysis of a SMT Solder Joint Using a Nonlinear FEM Approach", J. Microcircuits and Electron. Packaging, vol. 16, pp. 79-88.

Arrowood, R., A. Mukherjee, and W. B. Jones, 1991, "Solder Mechanics: A State of the Art Assessment", D. R. Frear, W. B. Jones, and K. R. Kinsman, eds., p. 107, The Minerals, Metals, and Materials Society, Warrendale, PA.

Busso, E. P., M. Kitano, and T. Kumazawa, "A viscoplastic constitutive model for 60/40 tin-lead solder used in IC package joints," J. Eng. Mat. Tech., 114, p. 331, 1992.

Busso, E. P., Kitano, M., Kumazawa, T., 1994, "Modeling Complex Inelastic Deformation Processes in IC Packages' Solder Joints", J. Electron. Packaging, vol. 116, pp. 6-15.

Clech, J-P., Englelmaier, 1989, W., Kotlowicz, R. W. and Augis, J. A., SMART Conf. V, New Orleans, LA.

Coffin, L. F., Jr., 1954, Trans. ASME V76, pp. 931-950.

Coffin, L. F., Jr., 1969, Fracture 1969, Chapman and Hall, London.

Darveaux, R., and K. Banerji, 1992, "Constitutive relations for tin-based solder joints," IEEE Trans. Components, Hybrids, and Manufacturing Tech., 15, pp. 1013-1024.

Dasgupta, A., Oyan, C., Barker, D., Pecht, M., 1992,

"Solder Creep-Fatigue Analysis by an Energy-Partitioning Approach", J. Electron. Packaging., vol. 114, pp. 152-160.

Frear, D. R., 1989, "Thermomechanical Fatigue of Solder Joints: A New Comprehensive Test Method" IEEE Comp. Hybrids. Manufact. Tech., CHMT-12, pp. 492-501.

Frear, D. R., 1992, "Microstructural Evolution During the Thermomechanical Fatigue of Solder Joints", in The Metal Science of Joining, Cieslak, Glicksman, Kang and Perepezko eds., TMS Publications, 191-200.

Frear, D. R., Rashid, M. M., Burchett, S. N., 1993, "Microstructurally Based Thermomechanical Fatigue Lifetime Model of Solder Joints for Electronic Applications", Reliability, Stress Analysis and Failure Prevention, DE-vol. 55, ASME, R. J. Schaller, ed., pp. 277-287.

Guo, Q., Cutiongco, E. C., Keer, L. M., Fine, M. E., 1992, "Thermomechanical Fatigue Life Prediction of 63Sn-37Pb Solder", J. Electron. Packaging, vol. 114, pp. 145-151.

Hacke, P., Sprecher, A. F., Conrad, H., 1993, "Computer Simulation of Thermomechanical Fatigue of Solder Joints Including Microstructure Coarsening", J. Electron. Packaging, vol. 115, pp. 153-158.

Huang, J. H., Pei, J. Y., Qian, Y. Y., Jiang, Y. H., 1994, "Life Predictions of SMT Solder Joints under Thermal Cycling", Soldering and Surface Mount Technol., vol. 16, 31-50.

Lau, J. H., 1993, "Thermal Fatigue Life Prediction of Flip Chip Solder Joints by Fracture Mechanics Method", Engineering Fracture Mechanics, vol. 45, pp. 643-654.

Lau, J., Erasmus, S., 1993, "Reliability of Fine Pitch Plastic Quad Flat Pack Leads and Solder Joints Under Bending, Twisting, and Thermal Conditions", J. Electron. Packaging, vol. 115, pp. 322-328.

Lee, S. M., 1993, "Creep and he Creep-Fatigue Interaction in Pb-Sn Eutectic and Eutectic Solder Joints", Ph.D. Thesis, The University of Wisconsin, Madison.

Manson, S. S., 1953, "Behavior of Materials Under Conditions of Thermal Stress", Heat Transfer Symposium, Univ. of Michigan, June 27-28,1952, Univ. of Mich. Press; also NACA TN2933.

Manson, S. S., 1960, Mech. Des. V32(14), pp. 139-

Pan, T.-Y., Winterbottom, W. L., 1990, "Thermal Cycling Induced Plastic Deformation in Solder Joints", ASME Winter Annual Meeting, Dallas, TX.

Pao, Y.-H., Govila, R., Badgley, S., Jih, E., 1993, "An Experimental and Finite Element Study of Thermal Fatigue Fracture of PbSn Solder Joints", J. Electron. Packaging, vol. 115, pp. 1-8.

Rohde, R. W., and J. C. Swearengen, "Deformation modeling applied to stress relaxation of four solder alloys," J. Eng. Mat. Tech., 102, pp. 207-214, 1980.

Ross, R. G., Wen, L. C., Mon, G. R., Jetter, E., 1992, "Solder Creep-Fatigue Interactions with Flexible Leaded Parts", J. Electron. Packaging, vol. 114, pp. 185-192.

Sandor, B. I., 1991, "Lifetime Prediction of Solder Joints: Engineering Mechanics Methods", in Solder Me-

chanics: A State of the Art Assessment, D. R. Frear, W. B. Jones, K. R. Kinsman, eds., TMS Publications, Warrendale, PA.

Sandstrom, R., Osterberg, J.-O., Nylen, M., 1993, "Deformation Behavior During Low Cycle Fatigue Testing of 60Sn-40Pb Solder", Materials Science and Technol., vol. 9, pp. 811-819.

Sauber, J., Seyyedi, 1992, "Predicting Thermal Fatigue Lifetimes for SMT Solder Joints", J. Electron. Packaging,

vol. 114, pp. 472-476.

Schmidt, C. G., 1992, "A Simple Model for Fatigue of Leadless Ceramic Chip Carrier Solder Attachments", J.

Electronics Manufac., vol. 2, pp. 31-36.

Solomon, H. D., 1994, "Life Prediction and Accelerated Testing", in The Mechanics of Solder Alloy Interconnects, D. R. Frear, H. S. Morgan, S. N. Burchett, J. Lau, eds., Van Nostrand Reinhold, New York, NY.

Stone, D. S., and M. M. Rashid, 1994, "Constitutive models," in "The Mechanics of Solder Alloy Interconnects", D. R. Frear, S. N. Burchett, H. S. Morgan, and J. H. Lau,

eds., pp. 87-157, Van Nostrand Reinhold.

Verma, S., Dasgupta, A., Barker, D., 1993, "A Numerical Study of Fatigue Life of J-Leaded Solder Joints Using the Energy Partitioning Approach", J. Electron. Packaging, vol. 115, pp. 416-423.

#### DISCLAIMER

This report was prepared as an account of work sponsored by an agency of the United States Government. Neither the United States Government nor any agency thereof, nor any of their employees, makes any warranty, express or implied, or assumes any legal liability or responsibility for the accuracy, completeness, or usefulness of any information, apparatus, product, or process disclosed, or represents that its use would not infringe privately owned rights. Reference herein to any specific commercial product, process, or service by trade name, trademark, manufacturer, or otherwise does not necessarily constitute or imply its endorsement, recommendation, or favoring by the United States Government or any agency thereof. The views and opinions of authors expressed herein do not necessarily state or reflect those of the United States Government or any agency thereof.